Journal of Nanophotonics

SPIEDigitalLibrary.org/jnp

Silicon-on-insulator microring resonator defect-based photodetector with 3.5-GHz bandwidth

Jason J. Ackert
Marco Fiorentino
Dylan F. Logan
Raymond G. Beausoleil
Paul E. Jessop
Andrew P. Knights

SPIE

Silicon-on-insulator microring resonator defect-based photodetector with 3.5-GHz bandwidth

Jason J. Ackert,[a] Marco Fiorentino,[b] Dylan F. Logan,[a] Raymond G. Beausoleil,[b] Paul E. Jessop,[c] and Andrew P. Knights[a]

[a] McMaster University, Department of Engineering Physics, 1280 Main St. West, John Hodgins Engineering Building, Room A315, Hamilton, ON L8S 4L8 Canada
ackertjj@mcmaster.ca

[b] Hewlett Packard Laboratories, 1501 Page Mill Road, Palo Alto, California

[c] Wilfrid Laurier University, Department of Physics, 75 University Avenue West, Waterloo, Canada

Abstract. We have devised and fabricated high-speed silicon-on-insulator resonant microring photodiodes. The detectors comprise a p-i-n junction across a silicon rib waveguide microring resonator. Light absorption at 1550 nm is enhanced by implanting the diode intrinsic region with boron ions at 350 keV with a dosage of 1×10^{13} cm^{-2}. We have measured 3-dB bandwidths of 2.4 and 3.5 GHz at 5 and 15 V reverse bias, respectively, and observed an open-eye diagram at 5 gigabit/s with 5 V bias.
[DOI: 10.1117/1.3666059]

Keywords: integrated optics; optical interconnects; silicon; photodetectors.

Paper 11106LR received Sep. 29, 2011; revised manuscript received Nov. 14, 2011; accepted for publication Nov. 16, 2011; published online Dec. 13, 2011.

1 Introduction

Silicon-on-insulator (SOI) is the platform of choice for integrated photonic interconnects, due to compatibility with complementary metal-oxide-semiconductor processes (CMOS) and the resulting low cost.[1,2] Although silicon's transparency in the infrared is well suited for low-loss waveguides, this presents difficulty for monolithically integrating photodetectors on a common substrate. Typically, other materials must be employed for detection, such as epitaxial germanium.[3]

Silicon can be made responsive to 1550 nm light with the use of lattice defect states introduced via ion implantation, a CMOS compatible process. This absorption may be exploited for subbandgap detection as described in the report by Logan et al.[4] in which the effect on detector performance of device geometry and defect concentration was presented. The high-speed performance of waveguide integrated detectors has been previously investigated by Geis et al.,[5] where the potential of this technology was demonstrated for use as a high-speed receiver diode. Silicon defect detectors have recently been incorporated into ring resonator structures based on ion-implanted silicon,[6,7] deposited silicon[8] and surface state defects.[9] The resonator geometry provides a compact device footprint, wavelength selectivity, and increased responsivity due to the buildup of optical intensity within the cavity. To date, only one report of device bandwidth has been made for an implanted silicon resonant detector with those preliminary results showing a 3-dB bandwidth of 7 GHz.[10] Relatively few details were provided in that work with regard to the limit in speed of operation. If these devices are to be utilized as a wavelength selective receiver, a greater understanding of their data-handling capability is required.

In this paper, we (*i*) present frequency response measurements for silicon defect-based detectors incorporated into a 20-μm-radius ring resonator, (*ii*) demonstrate an open eye at 5 gigabit/s, and (*iii*) discuss possible bandwidth limitations.

1934-2608/2011/$25.00 © 2011 SPIE

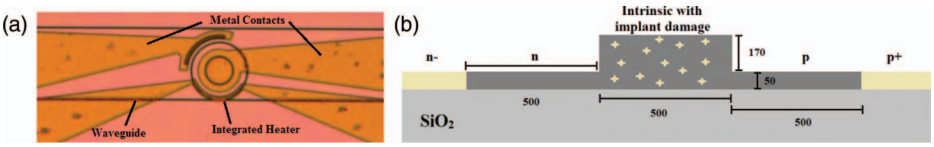

Fig. 1 (a) Optical micrograph of the resonant photodiode. The ring structure has a radius of 20 μm. The upper contacts form the photodiode, whereas the lower are an integrated heater (not utilized in this work). (b) A cross-sectional diagram of the p-i-n diode (in nanometers). Defects in the intrinsic region mediate photon absorption.

2 Device Fabrication

The devices were fabricated with the 193-nm-deep UV lithography process of CEA-LETI. The SOI wafers consisted of 220 nm top silicon on a 2-μm buried oxide. The waveguides were defined with a 170-nm etch, leaving a 50-nm silicon slab. A 1-μm oxide was deposited across the wafer to avoid optical absorption in the 560-nm-thick Al/Cu metal contact layer. The p-i-n diodes were created by phosphorous and boron doping at a dose of 2×10^{14} cm^{-2}. Boron ions at 350 keV, with a dosage of 1×10^{13} cm^{-2} were implanted in the intrinsic region to introduce defects in the lattice, which were subsequently annealed at 200°C for 5 min. These defects establish deep levels within the bandgap,[11] increasing optical absorption in the infrared.[12] An optical micrograph and cross-sectional diagram are shown in Fig. 1. Light was coupled into the chips from a single-mode fiber through 70 nm shallow etch transverse electric (TE) mode grating couplers designed for 1550 nm.[13] Through the use of passive test waveguides (adjacent to the resonant detector structures), the total loss of the device was approximated to be 16 dB. This measurement allowed a determination of the detector responsivity.

3 Device Characteristics

The p-i-n photodiodes were incorporated within 20-μm-radius rings as shown in Fig. 1. The rings had a nominal waveguide width of 500 nm and a coupling gap of 200 nm. The quality factor (Q) was measured to be approximately 10×10^3 and the free spectral range was 4.98 $\pm$ 0.02 nm. Figure 2 shows a wavelength scan of light coupled into the 20-μm-radius microring resonator. The photocurrent is greatly enhanced on resonance, and from an estimation of on chip

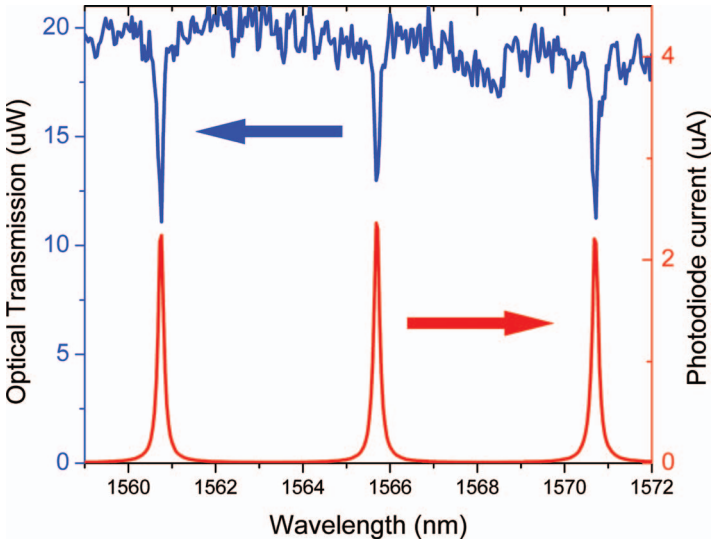

Fig. 2 Optical transmission and diode photocurrent as a function of wavelength for a 20-μm-radius microring resonator photodiode biased at –5 V.

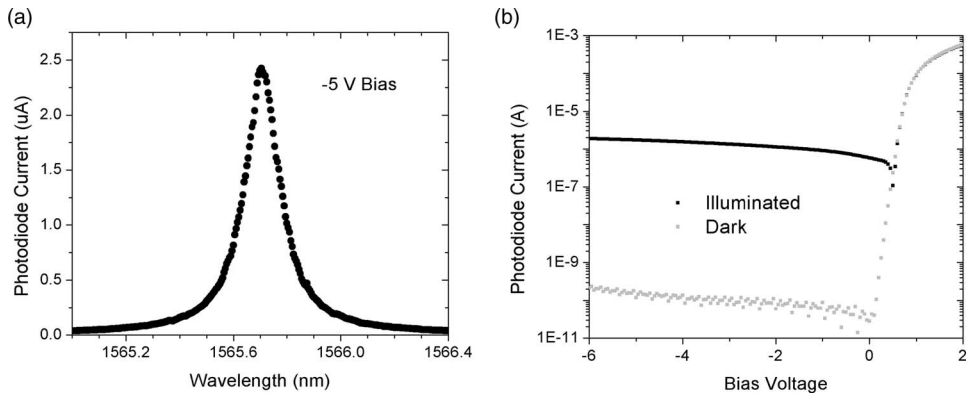

Fig. 3 (a) High-resolution wavelength scan of the photodiode resonance at –5 V. (b) Current versus voltage for the photodiode with and without coupled light. Waveguide-coupled optical power is estimated at 110 μW.

power, we calculate a responsivity of 0.023 A/W with a –5-V applied bias. In Fig. 3, a current versus voltage plot of the diode shows dark current below 0.2 nA at −5 V bias.

4 Measurement Methods

To measure the transient response of the photodetectors, a vector network analyzer was used in conjunction with a 10-GHz lithium niobate Mach–Zehnder modulator. A picosecond pulse lab 550B bias tee, rated at 18 GHz, was used to apply the bias voltage to the device under test. The response was calibrated with a 12-GHz commercial InGaAs detector, eliminating the frequency response of the system except for the probe assembly, which is a Picoprobe 40A-GS-300 rated at 40 GHz. To record the eye diagram, a 12.5 gigabit/s pulse pattern generator was used to drive the modulator, and a digital communications analyzer recorded the detector response after a 25-GHz amplifier. The power coupled into the waveguide for frequency response measurements was on the order of 0.5 mW. From the network analyzer, we observed a 3-dB bandwidth of ∼2 GHz at –5 V bias which is shown in Fig. 4. This increased to 3 GHz at –15 V, but further

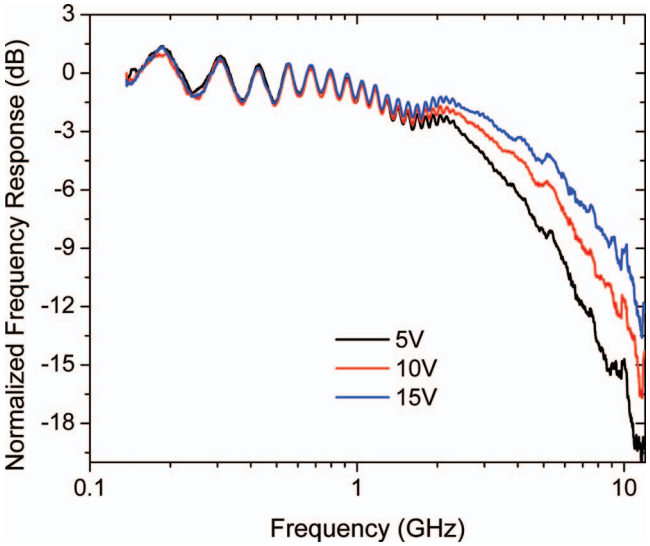

Fig. 4 Normalized frequency response of the microring detector for 5-, 10-, and 15-V reverse bias. As the bias is increased, the response increases from 2.4 to 3.5 GHz.

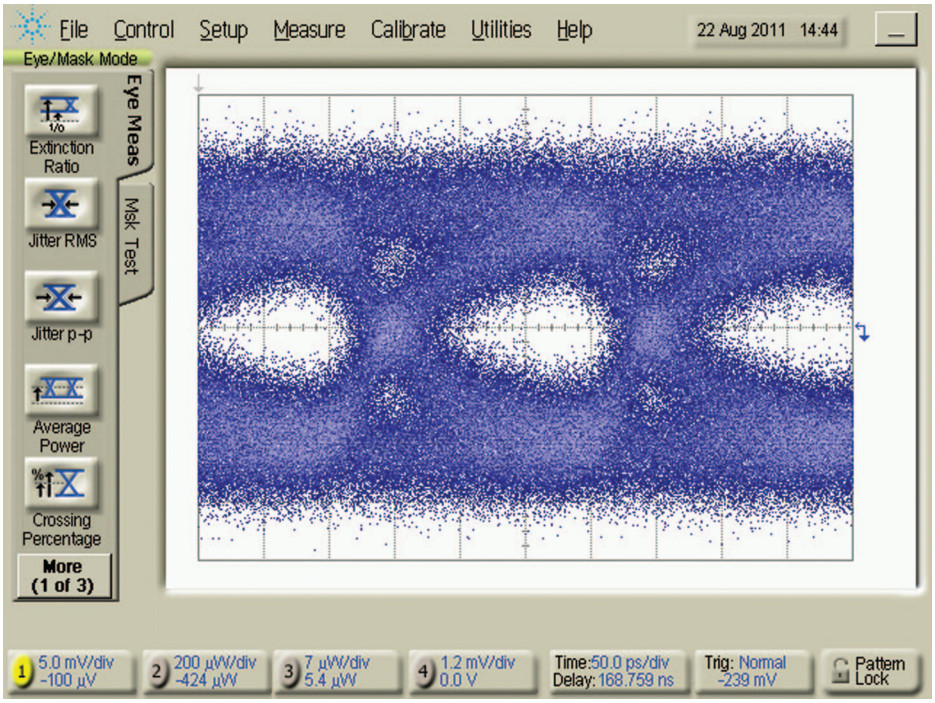

Fig. 5 Eye diagram from the microring detector. The photodiode was biased at –5 V and was receiving a 5-gigabit/s pseudorandom binary sequence (PRBS $2^{31} - 1$).

bias increases had no effect. An open eye was observed for a 5-gigabit/s pattern with the diode biased at –5 V (shown in Fig. 5).

5 Discussion

Although achieving over 2-GHz operation at a modest bias of 5 V, these detectors operate below the speed of the photodiodes demonstrated by Shafiiha et al.[10] We note that there were significant differences in the implantation conditions and subsequent thermal annealing between the devices reported here and those of Ref. 10. The devices reported by Shafiiha et al.[10] incorporated defects through similar implantation and annealing conditions used in the nonresonant devices produced by Geis et al.[5] such that interstitial clusters were reported to be the optically active defect. The relatively high postimplantation annealing temperature used in Refs. 5 and 10 would rule out the presence of divacancy defects, whereas the devices reported here received a boron implantation followed by a 200°C anneal. For these conditions, the active optical defect is understood to be the divacancy.

Although the nature of the defects may well impact operational bandwidth, there are other factors that also require consideration. If the Q of the resonator is too high, then the bandwidth will be limited by a long photon lifetime, but a Q of 10×10^3 (as for our devices) imposes a limit of 19 GHz. There is a need to also consider the device capacitance as a limit in detector bandwidth. The capacitance of the ring diode was found to near the edge of sensitivity for our test equipment, a Boonton 7200 capacitance meter. To verify this result and achieve an accurate value, we measured multiple lengths of nonresonant test structures that shared the same doping profile and waveguide design as the ring diode. From this approach, we estimate the capacitance of this device to be 25 ± 10 fF, which would not, in principal, limit the bandwidth at $<$100 GHz. Another possibility is that the device is limited by carrier transit time. If we assume the thermal saturation velocity of carriers is reached at –15-V bias, then the bandwidth limitation should not be less than 21 GHz. These three effects obviously impose limits well above the

measured response. More work is thus required to determine the impact of device design and defect structure on the detector bandwidth.

6 Summary

SOI microring-defect photodetectors have been fabricated and their 3-dB bandwidth has been found to be 3.5 GHz at –15-V bias and 2.4 GHz at –5-V bias. Although the incorporation of monolithic silicon diodes in a microring resonator offers the potential for use in wavelength-division-multiplexed (WDM) links, the nature of the limitation on the device bandwidth remains elusive at this time.

Acknowledgments

The authors thank Dan Deptuck, CMC Microsystems and CEA-LETI, for facilitating the device design and fabrication. We also thank Greg Wojcik and Feng Zhang, of Innolume Inc., for discussion and assistance with equipment.

This paper was authored by J. J. Ackert, who also performed device characterization with M. Fiorentino while under management of R. G. Beausoleil at Hewlett Packard Laboratories. D. F. Logan designed the device, while A. P. Knights and P. E. Jessop provided supervision, discussion of the results and funding for the work.

References

1. L. Pavesi and G. Guillot, *Optical Interconnects: The Silicon Approach*, Springer-Verlag, Berlin (2006).
2. R. G. Beausoleil, "Large scale integrated photonics for high performance interconnects," *ACM J. Emerging Technol. Comput. Syst.* **7**(2), article 6 (2011).
3. J. Michel, J. Liu, and L. C. Kimerling, "High-performance Ge-on-Si photodetectors," *Nat. Photon.* **4**(8), 527–534 (2010).
4. D. F. Logan, P. E. Jessop, and A. P. Knights, "Modelling defect enhanced detection at 1550 nm in Integrated silicon waveguide detectors," *J. Lightwave Technol.* **27**(7), 930–937 (2009).
5. M. W. Geis, S. J. Spector, M. E. Grein, J. U. Yoon, D. M. Lennon, and T. M. Lyszczarz, "Silicon waveguide infrared photodiodes with >35 GHz bandwidth and phototransistors with 50 AW^{-1} response," *Opt. Express* **17**(7), 5193–5204 (2009).
6. D. F. Logan, P. Velha, M. Sorel, R. M. De La Rue, A. P. Knights, and P. E. Jessop, "Defect-enhanced silicon-on-insulator waveguide resonant photodetector with high sensitivity at 1.55 μm," *IEEE Photon. Technol. Lett.* **22**(20), 1530–1532 (2010).
7. J. K. Doylend, P. E. Jessop, and A. P. Knights, "Silicon photonic resonator-enhanced defect-mediated photodiode for sub-bandgap detection," *Opt. Express* **18**(14), 14671–14678 (2010).
8. K. Preston, Y. H. D. Lee, M. Zhaing, and M. Lipson, "Waveguide-integrated-telecom photodiode in deposited silicon," *Opt. Lett.* **36**(1), 52–54 (2011).
9. H. Chen, X. Luo, and A. W. Poon, "Cavity-enhanced photocurrent generation by 1.55 μm wavelengths linear absorption in a p-i-n diode embedded silicon microring resonator," *Appl. Phys. Lett.* **95**, 171111 (2009).
10. R. Shafiiha, D. Zheng, S. Liao, P. Dong, H. Liang, N. Feng, B. J. Luff, D. Feng, G. Li, J. Cunningham, K. Raj, A. V. Krishnamoorthy, and M. Asghari, "Silicon waveguide coupled resonator infrared detector," in *Proc. of Optical Fiber Communication Conf./Natl. Fiber Optic Engineers Conf.*, Paper No. OMI8 (2010).
11. S. Libertino and A. La Manga *Damage Formation and Evolution in Ion-Implanted Crystalline Si*, Topics in Applied Physics, Springer-Verlag, Berlin (2010).

12. P. J. Foster, J. K. Doylend, P. Mascher, A. P. Knights, and P. G. Coleman, "Optical attenuation in defect engineered silicon rib waveguides," *J. Appl. Phys.* **99**(7), 073101 (2006).
13. D. Taillaert, F. Van Laere, M. Ayre, W. Bogaerts, D. Van Thourout, P. Bientsman, and R. Baets, "Grating couplers for coupling between optical fibers and nanophotonic waveguides," *Jpn. J. Appl. Phys.* **45**(8A), 6071–6077 (2006).

Biographies and photographs of authors not available.